VIP Fungal Natural Products Very Important Paper

International Edition: DOI: 10.1002/anie.201910175
German Edition: DOI: 10.1002/ange.201910175

Injury-Triggered Blueing Reactions of *Psilocybe* "Magic" Mushrooms

*Claudius Lenz[+], Jonas Wick[+], Daniel Braga, María García-Altares, Gerald Lackner, Christian Hertweck, Markus Gressler, and Dirk Hoffmeister**

Abstract: *Upon injury, psychotropic psilocybin-producing mushrooms instantly develop an intense blue color, the chemical basis and mode of formation of which has remained elusive. We report two enzymes from Psilocybe cubensis that carry out a two-step cascade to prepare psilocybin for oxidative oligomerization that leads to blue products. The phosphatase PsiP removes the 4-O-phosphate group to yield psilocin, while PsiL oxidizes its 4-hydroxy group. The PsiL reaction was monitored by in situ ^{13}C NMR spectroscopy, which indicated that oxidative coupling of psilocyl residues occurs primarily via C-5. MS and IR spectroscopy indicated the formation of a heterogeneous mixture of preferentially psilocyl 3- to 13-mers and suggest multiple oligomerization routes, depending on oxidative power and substrate concentration. The results also imply that phosphate ester of psilocybin serves a reversible protective function.*

Mushrooms from the genus *Psilocybe* accumulate psilocybin (**1**, Scheme 1), which makes them strongly hallucinogenic.[1] As a rare reaction among natural product biosyntheses, **1** assembly includes a phosphotransfer step, catalyzed by the kinase PsiK.[2] Upon ingestion of the mushrooms, the phosphate ester is cleaved to yield psilocin (**2**), the actual psychotropic congener that profoundly alters human perception by binding agonistically to 5-hydroxytryptamine receptors.[3] Ecologically, the presence of monomeric **1** in the fungus has been attributed to protection from mycophagous insects by interfering with their behaviour.[4] A second very prominent phenomenon is the blueing reaction of *Psilocybe* mushrooms, reflected by species names such as *P. cyanescens* or *P. azurescens*. Upon bruising or cutting, **1**-containing fruiting bodies instantaneously develop a dark blue color at the site of injury (Figure 1, Movie S1). Likewise, *Psilocybe* specimens may turn blue as they age. A blue coloration that instantly develops upon injury is observed with other mushrooms as well. In the case of the dotted stem bolete[5] and the cornflower mushroom, the blueing can be attributed to pulvinic acid or diarylcyclopentenone derivatives.[6]

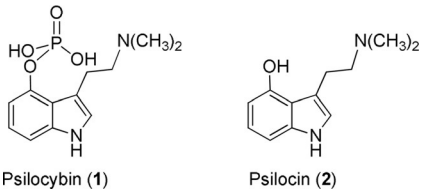

Scheme 1. Chemical structures of psilocybin (**1**) and psilocin (**2**).

Figure 1. The blueing reaction of *Psilocybe cubensis*: intact (left) and scalpel-injured mushroom (right).

However, the structure of the chromophore and the biochemical basis how this blue pigment is formed in *Psilocybe* has remained elusive, although this conundrum has attracted natural product chemists' attention for decades.[7,8] When oxidized chemically, for example, by ferric iron or base,[1c] or enzymatically, **2** but not **1** is converted to a blue pigment.[7] It has been hypothesized that the chromophore is most likely a **2**-derived *ortho*-coupled biarylidenedione.[8] Furthermore, the existence of a stable radical was assumed.[7d,8] Precedence exists for enzymatic biaryl coupling in fungal natural products, catalyzed by cytochrome P450 or flavin-dependent monooxygenases, or laccases whose selectivity may be intrinsic or conferred by auxiliary proteins.[9]

[*] C. Lenz,[+] Dr. J. Wick,[+] Dr. M. Gressler, Prof. Dr. D. Hoffmeister
Department Pharmaceutical Microbiology, Hans-Knöll-Institute
Friedrich-Schiller-Universität
Beutenbergstr. 11a, 07745 Jena (Germany)
E-mail: dirk.hoffmeister@leibniz-hki.de

Dr. D. Braga, Dr. G. Lackner
Synthetic Microbiology, Friedrich-Schiller-Universität, Leibniz Institute for Natural Product Research and Infection Biology – Hans-Knöll-Institute, Winzerlaer Str. 2, 07745 Jena (Germany)

Dr. M. García-Altares, Prof. Dr. C. Hertweck
Department Biomolecular Chemistry, Leibniz
Institute for Natural Product Research and Infection Biology – Hans-Knöll-Institute, Beutenbergstr. 11a, 07745 Jena (Germany)

[+] These authors contributed equally to this work.

Supporting information and the ORCID identification number(s) for the author(s) of this article can be found under: https://doi.org/10.1002/anie.201910175.

The presence of reducing agents, such as sodium dithionite, has been shown to discolor the blue matter, which is reversible upon re-oxidation, thus supporting the notion of a quinoid chromophore.[7c] In the presence of a phosphatase, a blue color develops from **1** as well.[10] Sequential **1** degradation through dephosphorylation, oxidation, and subsequent oligomerization would explain the rapid bluing reaction of *Psilocybe* mushrooms. In this work, we address this long-standing problem with a combined approach primarily based on activity-guided chromatographic purification of a phosphatase (PsiP) and a laccase (PsiL) of *P. cubensis* that carry out a two-step degradative cascade to convert **1** into **2**, which then undergoes oligomerization (Scheme 2). MALDI-MS and LC-MS, IR spectroscopy, and in situ time-resolved NMR spectroscopy provided insight in the oligomerization modes.

We used *P. cubensis* carpophores to isolate native enzymes by protein chromatography (Figure S1). After each chromatographic step, in vitro activity assays were performed. Phosphatase activity was traced using **1** as an authentic substrate for the production of **2**, and 4-nitrophenyl dihydrogen phosphate as a chromogenic standard substrate. To detect oxidase activity, **2** and syringaldazine were used in parallel as substrates to yield photometrically detectable products. Cell extracts were first subjected to anion-exchange chromatography (AIEC). Then, positively assayed fractions were further separated by hydrophobic interaction (HIC) and size-exclusion chromatography (SEC).

Active SEC fractions were tryptically digested and subjected to MS/MS-based peptide fingerprinting. Using the deduced proteome of *P. cubensis* as a search database, the fraction containing the phosphatase activity revealed six candidates (Table S1 in the Supporting Information). Consistently, the highest-ranking protein (JGI ProteinID 89927) was annotated as a phosphatase. Another candidate phosphatase (JGI ProteinID 74822) displayed a much lower intensity and a lower identification score (Figure S2) and could not be detected reproducibly. The first putative phosphatase (PsiP) is a member of the histidine acid phosphatase superfamily. The DNA sequence encoding PsiP (552 aa, calculated mass of 59.5 kDa, Table S2) was localized in the *P. cubensis* genome and was not associated with **1** biosynthesis genes. Bioinformatic analysis pointed to a lysosomal localization of PsiP (Figure S3, Table S3). Of note, other **1**-producing mushrooms encode extremely similar phosphatases (Table S4). LC-MS analyses and an authentic standard demonstrated that PsiP dephosphorylates **1** to **2**. Signals of identical mass, retention time ($t_R = 2.15$ min), and UV/Vis spectra were observed (Figure 2). We therefore describe PsiP as **1** phosphatase.

Peptide mass fingerprinting of the fraction with oxidizing activity identified seven candidate proteins (Table S5 and Figure S4). One of the top scoring proteins was annotated as a multicopper oxidase (JGI ProteinID 71514) according to Pfam[11] and InterPro[12] domain analyses and was similar to a laccase, that is, a multi-copper oxidases that catalyze removal of one electron from the target substrate.[13] In addition to displaying 10 high-intensity peptides with strong MS/MS support, the putative laccase, now referred to as PsiL,

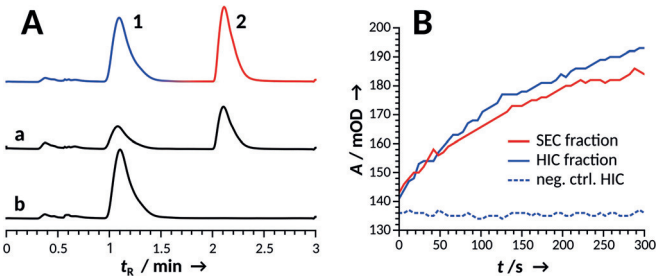

Figure 2. Analysis of in vitro reactions. A) Top trace (composite individual chromatograms): authentic standards of **1** and **2**. Trace a: PsiP (SEC fraction) catalyzing **1** dephosphorylation. Trace b: negative control with heat-denatured enzyme. B) Typical PsiL-dependent blueing reaction with **2** as the substrate, measured photometrically as absorbance at $\lambda = 618$ nm. $t = 0$ reflects the first measurement of absorption. The time delay between substrate addition and first photometric measurement is approx. 30 s. The negative control was run with a heat-treated HIC fraction containing laccase.

was the only identified protein with an annotation that provides a reasonable explanation for the expected radical oxidation reaction. The *psiL* gene was identified but, like *psiP*, it is not located in the **1** biosynthesis gene cluster. The *psiL* gene (Table S2) encodes a 528 aa protein with a calculated mass of 57.5 kDa that shows 63% amino acid identity to a yellow laccase of the mushroom *Stropharia aeruginosa* (GenBank accession code: AFE48786.2).[14] PsiL is likely an extracellular enzyme (Figure S3), and PsiL-like laccases (61–71% identical aa) are encoded in all **1**-producing fungi whose genomes are available (Figure S5 and Table S6). Optimum reaction parameters were determined both for PsiL and PsiP (Figure S6).

Oxidizing activity on **2**, but not on **1**, was observed for PsiL based on a photometrically detected blue color (Figure 2) which was absent in a control with heat-treated enzyme. The activity of PsiL was comparable to *Myceliophthora thermophila* laccase, yet three orders of magnitude above a *Trametes* laccase (Figure S7, Table S7). We therefore conclude that PsiP initiates and PsiL continues an enzymatic pathway to convert **1** into a **2**-based polymeric colored material.

PsiL-analogous model reactions for chemical (Fe^{III}) or enzymatic oxidation (*M. thermophila* laccase/O_2 or horseradish peroxidase (HRP)/H_2O_2) were set up to produce the blue color and analyze **2** oxidation. In both cases, LC-MS traces showed decreased **2** content and formation of the blue color without noticeable qualitative or quantitative differences. When oxidized with Fe^{III}, that is, in a protein-free environment, the blue compound was amenable to characterization by MALDI-MS and LC-MS. However, when oxidized enzymatically, the majority of colored product was chromatographically inseparable and adhered to proteins, as previously reported.[7d] The MALDI-TOF mass spectra revealed a complex pattern of discrete signals representing multiples of m/z 202, that is, the mass-to-charge ratio of **2** monomers less two protons, thus indicating oligomerization up to 13-mers, accompanied by a consistent pattern of co-occurring ions (Figure S8). Smaller oligomers were analyzed by LC-MS, which verified dehydro- and primarily didehydro-coupling

products, and oxidized derivatives thereof (Figure S9). The complexity of the product mixture was reduced by replacing water with methanol as the solvent, and by diluting and cooling. Then, a clear blue solution was obtained that predominantly contained the didehydro dimer of **2** (*m*/*z* 405), which shows absorptivity around 600 nm. Its leuco form, a colorless **2** dehydrodimer (*m*/*z* 407), was reversibly generated by lowering the redox potential of the solution, for example, by addition of $Na_2S_2O_4$ or EDTA (Figure S10). Concurrently, IR spectra of blue oligomeric and polymeric product fractions were recorded (Figure S11). The spectra show similarities with those of eumelanin,[15] featuring strong O–H and N–H stretching bands between 3,500 and 3,100 cm^{-1}, and distinct signals in the range of conjugated C=O and C=C bonds (1,610 and 1,641 cm^{-1}).

While these features become less defined in the polymeric fraction spectrum, absorptions of various C–H, C–O, C–C and N–H vibrations (3,100–2,700 cm^{-1} and fingerprint region) increased, probably due to both higher structural inhomogeneity and degree of polymerization, as shown for substrate concentration variation in laccase-mediated coupling of 3-methylcatechol.[16]

The finding of carbonyl functions and oligomeric, 2H-spaced mass clusters (e.g. *m*/*z* 405–407 $[M+H]^+$), combined with reversible Fe^{III}-mediated redox chemistry, suggests initial formation of biindolidene quinonic products, as proposed previously.[8] Subsequently, MS was used to compare with the enzymatic reaction. A diluted laccase/O_2 oxidation of **2** was repeatedly and directly subjected to LC-MS (Figure 3, Figure S12). As the substrate **2** was gradually consumed and the blue color concurrently formed, dimeric **2** (*m*/*z* 405–407) became less abundant over time while masses of higher oligomers appeared.

We further characterized **2** autoxidation by LC-MS, which indicated oligomerization as well. However, in aqueous buffers, the color ranged from greenish to taupe or brown (Figure S10). Prominent product ions include *m*/*z* 219 (**2** + [O] −2[H]), 419 (dimeric **2** + [O] −6[H]), and 621 (trimeric **2** + [O] −8[H]). With higher concentrations of **2**, increasing amounts of ion *m*/*z* 407, but not *m*/*z* 405, were detected. For all detected product species, the expected sum formulae were confirmed by HRMS (Table S8). The most prominent ones were analyzed by MS/MS to verify the presence of intact dimethylaminoethyl sidechains. The observed differences between autoxidation and chemically boosted or enzyme-mediated oxidation may be attributed to different mechanisms and pathways (Figure S13), that both originate from psilocyl radicals. Boosted oxidations produce an excess of radicals that enable direct radical coupling and subsequent oxidation of hydroquinoid compounds, which would explain the blue quinoid dimer (*m*/*z* 405). Autoxidation yielded low radical concentrations, where the average lifetime of the psilocyl radical may be insufficient to find a suitable radical coupling partner. In this scenario, psilocyl cations may be formed,[17] which would favor reactions driven by nucleophilic attacks to yield compounds such as *m*/*z* 219, 419, and others.

At this stage, MS had provided valuable information about general patterns of product formation. However, product complexity, product binding to proteins, polymerization, and autoxidation prevented purification of the individual products to homogeneity. We thus resorted to in situ NMR spectroscopy to monitor the progress of the enzymatic reaction. Buffered **2** solutions in D_2O (5 mg mL^{-1}) were oxidized enzymatically. For comparison, autoxidation of **2** by O_2 from an airstream supplied to an enzyme-free solution was monitored as well. For in situ ^1H and ^{13}C NMR spectroscopy, reactions were run directly in the spectrometer, recording ^1H NMR spectra every 2–3 minutes. Under autoxidation conditions, the signal of H-5 decreased by about 70% within 4 h. After 24 h, signal H-5 had virtually disappeared, the overlapping signals of H-6 and H-7 had decreased by about 30%, while all other protons were only marginally affected (Figure S14). However, no substantial substrate turnover within the same time was observed in LC-MS control measurements. Thus, the selective signal decrease must be based on an H/D-exchange with the solvent *ortho* (and to a lesser extent *para)* to the hydroxy functionality due to tautomerism.

We therefore proceeded with inverse-gated decoupling (igd) ^{13}C NMR of $^{13}C_{12}$-**2** to monitor the reaction. When HRP/

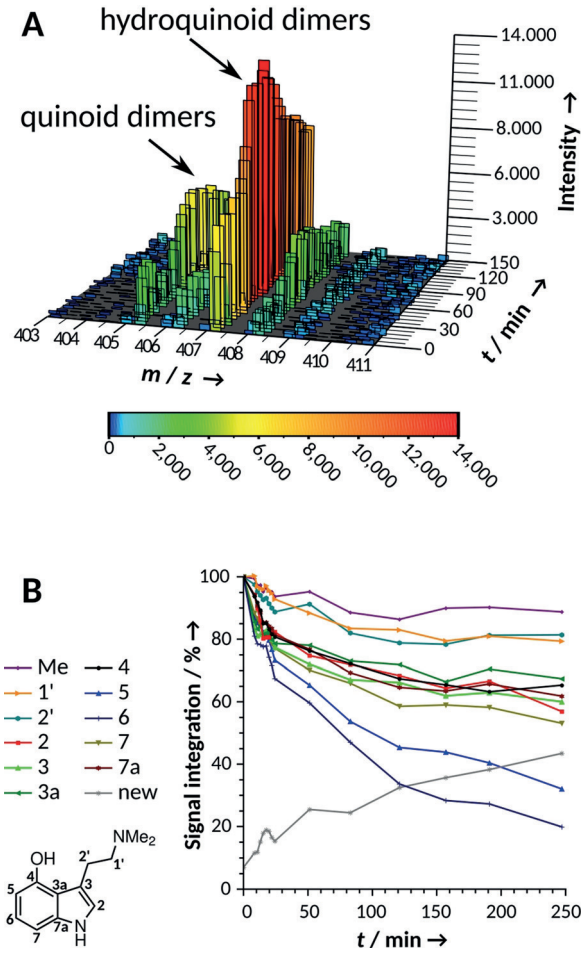

Figure 3. Chemical analysis of the blueing reaction. A) LC-MS-analysis of laccase-mediated **2** oxidation and concomitant formation and decrease of reduced or quinoid psilocyl dimers (*m*/*z* 405–407). B) Carbon signal intensity during **2** oligomerization, measured by in situ ^{13}C NMR spectroscopy. The positions are color-coded. "New" refers to an emerging signal, likely C-6.

H_2O_2 was used for oxidation, a blue color developed instantly after mixing. However, after approx. 30–60 min, the blue color faded and gradually turned into a light brown (Figure S10). Signal changes in the igd-^{13}C NMR spectra revealed distinct differences between the individual carbons of **2** (Figures 3 and Figure S15). The sidechain carbons (Me, C-1′, C-2′) were affected least while indole core carbon signals markedly decreased. The H-bound carbons of the six-membered ring were most affected (C-6 > C-5 > C-7). Additionally, a new signal was observed (putative dd or t at $\delta =$ 123.1 ppm). We conclude that the reaction primarily favors couplings via C-5 and secondly at C-7. Since the newly closed C–C bonds via C-5 and C-7 affect the signal of C-6 as expected, its strong decrease is in accordance with this assumption. Additionally, the new signal is likely due to the former 6-position with adjacently formed C–C bonds at C-5 and C-7.[18]

With mass spectrometric evidence for oxidative coupling of **2**, IR spectra indicating C=O and C=C functionalities, and NMR spectroscopy suggesting C-5 as a preferred coupling position, our findings strongly support the hypothesis of 5-5′ coupled quinoid subunits being responsible for the blue color of oxidation products of **2**,[8] and, hence, wounded *Psilocybe* mushrooms. The reported stable radical properties of the blue product[7d] are consistent with our findings, since semiquinones are the radical intermediates between quinones and hydroquinones detected during our study.[19] Likewise, semiquinoids exist within eumelanins, a biological polymer that shares, to a degree, structural features with polymeric **2**. However, no single blue compound exists in *Psilocybe* mushrooms. Various oxidative pathways contribute, to different extents, to the reaction. Each of them produces various chemical (including isomeric) species. Similar phenomena are known from the (aut)oxidation of phenolic and indolic substances.[18,20,21] The substrate to oxidant ratio seems to affect the mechanism and color (Scheme 2, Table 1).

Natural products, among them polyenes, cyanohydrins, and numerous others, serve as defense compounds or precursors that are formed after injury.[22] To this end,

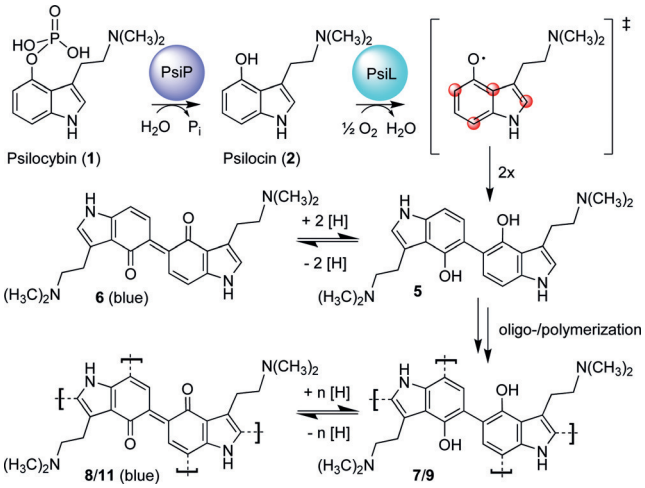

Scheme 2. The blueing reaction in *P. cubensis*, catalyzed by PsiP and PsiL. Stabilized electron positions within the psilocyl radical are highlighted in red. Numbering of compounds corresponds to Figure S13.

nature has evolved strategies to remove a protection group from an accumulated stable precursor. This initiates formation of the ecologically relevant monomeric defensive compound. Cyanide-releasing plant glycosides or mushroom metabolites, such as amygdaline or aleurodisconitrile,[22a] follow a similar strategy to quickly provide a wound-activated chemical defense when needed. However, such reactions require permanent physical separation of precursor and enzyme(s) that catalyze the cascade to convert the precursor into the actual defensive compound. Furthermore, they are triggered only upon injury, but ensure rapid product formation. In the case of *Psilocybe* mushrooms, this requires spatial separation of **1** and PsiL/PsiP for self-protection and to prevent polymerization and fatal protein crosslinking in intact cells. The sequences of PsiL and PsiP suggest extracellular or lysosomal localization, respectively (Table S3, Figure S3). Even though **2** is not the biosynthetic precursor of **1**, the kinase PsiK can rephosphorylate **2** to **1**.[2] Thus, PsiK adds

Table 1: Primary ion species detected by LC-MS, generated under various oxidation conditions (see also Table S8 and Figure S13). Structural isomers may occur.

Type	*m/z* (t_R in min)	Annotation	Neutral sum formula	Observed color	Mechanism[a]
Fe^{III}- or laccase-mediated oxidation[b]	405 (3.57)	Quinoid dimer **6**	$C_{24}H_{28}O_2N_4$	blue	R
	407 (3.38)	Hydroquinoid dimer **5**	$C_{24}H_{30}O_2N_4$	colorless	R
	607 (4.09)[c]	Quinoid trimer **8**	$C_{36}H_{42}O_3N_6$	blue	R
	609 (3.80)[c]	Hydroquinoid trimer **7**	$C_{36}H_{44}O_3N_6$	colorless	R
	807 (3.87)[c]	Fully quinoid tetramer **11**	$C_{48}H_{54}O_4N_8$	blue	R
	809 (3.93)[c]	Hybrid tetramer **10**	$C_{48}H_{56}O_4N_8$	blue/colorless	R
	811 (3.67)[c]	Hydroquinoid tetramer **9**	$C_{48}H_{58}O_4N_8$	colorless	R
Autoxidation	219 (3.53)[c]	Quinoid psilocin **16**	$C_{12}H_{14}O_2N_2$	brownish	N
	407[d] (3.38)	Hydroquinoid dimer **5**	$C_{24}H_{30}O_2N_4$	brownish	R
	419[e] (3.89)	Oxoquinoid dimer **19**	$C_{24}H_{26}O_3N_4$	greenish/brownish	N or R+N
	421[e] (3.28)	Hydroxyquinoid dimer **18a,b**	$C_{24}H_{28}O_3N_4$	greenish/brownish	N or R+N

[a] Plausible mechanism: R = direct radical coupling (Figure S13 II), R+N = nucleophilic addition on former radical coupling products (Figure S13 IV), N = nucleophilic addition (Figure S13 V). [b] Excess of oxidant favors quinoid species, oxidant deficiency favors hydroquinoid species. [c] Isomers detected, retention time indicates most intensive peak. [d] Abundant with higher **2** concentrations (25 mM). [e] Abundant with lower **2** concentrations (1 mM).

another layer of self-protection through its capacity to remove **2**. Oligo- and polymeric **2** consists of an extended conjugated system and, in the reduced state, numerous hydroxy groups that are oxidation-prone. Strikingly, these structure elements are similar to those of anti-oxidative compounds, such as flavonoids and polyphenolic tannins.[23] In the basic and oxidative environment of insect guts, such compounds act as producers of reactive oxygen species and can thus create intestinal lesions, which is presumably their main mode of toxic action.[24] Therefore, polymeric **2** may serve a defense function.

Our results shed light on the blueing reaction of *Psilocybe* mushrooms. We identified a laccase and a phosphatase that degrade **1** and initiate blueing in *P. cubensis*. MALDI-MS and in situ ^{13}C NMR spectroscopy show that the blue color is due to a heterogeneous mixture of quinoid psilocyl oligomers, primarily coupled via C-5. Our results further suggest that kinase-mediated phosphorylation during **1** biosynthesis reversibly deactivates a reactive natural product, and stabilizes it with an easily removable protection group that allows instant on-demand formation of an oligomeric natural product.

Acknowledgements

We thank A. Pschibul, A. Perner, H. Heinecke and S. Schieferdecker (Leibniz Institute for Natural Product Research and Infection Biology, Hans-Knöll-Institute Jena) for providing syringaldazine and *M. thermophila* laccase, and for recording HRMS and NMR spectra, respectively. We also thank J. Greßler (Friedrich-Schiller-University Jena) for technical assistance. C.L. acknowledges a doctoral fellowship by the International Leibniz Research School (ILRS) for Microbial Interactions. G.L. and D.B. thank the Carl Zeiss Foundation for funding. This work was supported by the Deutsche Forschungsgemeinschaft (DFG, grant HO2515/7-1). C.H. and D.H. are supported by the DFG Collaborative Research Center 1127 (ChemBioSys).

Conflict of interest

The authors declare no conflict of interest.

Keywords: enzymes · laccase · natural products · phosphatase · psilocybin

How to cite: *Angew. Chem. Int. Ed.* **2020**, *59*, 1450–1454
Angew. Chem. **2020**, *132*, 1466–1470

[1] a) A. Hofmann, R. Heim, A. Brack, H. Kobel, *Experientia* **1958**, *14*, 107–109; b) A. Hofmann, A. Frey, H. Ott, T. Petrzilka, F. Troxler, *Experientia* **1958**, *14*, 397–399; c) A. Hofmann, R. Heim, A. Brack, H. Kobel, A. Frey, H. Ott, T. Petrzilka, F. Troxler, *Helv. Chim. Acta* **1959**, *42*, 1557–1572.

[2] a) J. Fricke, F. Blei, D. Hoffmeister, *Angew. Chem. Int. Ed.* **2017**, *56*, 12352–12355; *Angew. Chem.* **2017**, *129*, 12524–12527.

[3] a) T. Passie, J. Seifert, U. Schneider, H. M. Emrich, *Addict. Biol.* **2002**, *7*, 357–364; b) F. Tylš, T. Páleníček, J. Horáček, *Eur. Neuropsychopharmacol.* **2014**, *24*, 342–356.

[4] a) H. T. Reynolds, V. Vijayakumar, E. Gluck-Thaler, H. B. Korotkin, P. B. Matheny, J. C. Slot, *Evol. Lett.* **2018**, *2*, 88–101; b) A. R. Awan, J. M. Winter, D. Turner, W. M. Shaw, L. M. Suz, A. J. Bradshaw, T. Ellis, B. Dentinger, *BioRxiv* **2018**, https://doi.org/10.1101/374199.

[5] W. Steglich, U. Furtner, A. Prox, *Z. Naturforsch. B* **1968**, *23*, 1044–1050.

[6] H. Besl, A. Bresinsky, W. Steglich, K. Zipfel, *Chem. Ber.* **1973**, *106*, 3223–3229.

[7] a) H. Blaschko, W. G. Levine, *Biochem. Pharmacol.* **1960**, *3*, 168–169; b) H. Blaschko, W. G. Levine, *Br. J. Pharmacol.* **1960**, *15*, 625–633; c) S. M. Bocks, *Phytochemistry* **1967**, *6*, 1629–1631; d) W. G. Levine, *Nature* **1967**, *215*, 1292–1293; e) J. Gartz, *Biochem. Physiol. Pflanzen* **1986**, *181*, 117–124.

[8] H. Laatsch in *Yearbook of the European College for the Study of Consciousness 1997* (Eds.: H.-C. Leuner, M. Schlichting), Verlag für Wissenschaft und Bildung, Berlin, **1998**, pp. 241–256.

[9] a) L. Fürtges, S. Obermaier, W. Thiele, S. Foegen, M. Müller, *ChemBioChem* **2019**, *20*, 1928–1932; b) S. Obermaier, W. Thiele, L. Fürtges, M. Müller, *Angew. Chem. Int. Ed.* **2019**, *58*, 9125–9128; *Angew. Chem.* **2019**, *131*, 9223–9226; c) S. Obermaier, M. Müller, *Biochemistry* **2019**, *58*, 2589–2593.

[10] A. Horita, L. J. Weber, *Biochem. Pharmacol.* **1961**, *7*, 47–54.

[11] R. D. Finn, P. Coggill, R. Y. Eberhardt, S. R. Eddy, J. Mistry, A. L. Mitchell, S. C. Potter, M. Punta, M. Qureshi, A. Sangrador-Vegas, G. A. Salazar, J. Tate, A. Bateman, *Nucleic Acids Res.* **2016**, *44*, D279–D285.

[12] P. Jones, D. Binns, H. Y. Chang, M. Fraser, W. Li, C. McAnulla, H. McWilliam, J. Maslen, A. Mitchell, G. Nuka, S. Pesseat, A. F. Quinn, A. Sangrador-Vegas, M. Scheremetjew, S. Y. Yong, R. Lopez, S. Hunter, *Bioinformatics* **2014**, *30*, 1236–1240.

[13] P. Baldrian, *FEMS Microbiol. Rev.* **2006**, *30*, 215–242.

[14] M. Daroch, C. A. Houghton, J. K. Moore, M. C. Wilkinson, A. J. Carnell, A. D. Bates, L. A. Iwanejko, *Enzyme Microb. Technol.* **2014**, *58–59*, 1–7.

[15] G. Perna, G. Palazzo, A. Mallardi, V. Capozzi, *J. Lumin.* **2011**, *131*, 1584–1588.

[16] C. Engelmann, S. Illner, U. Kragl, *Process Biochem.* **2015**, *50*, 1591–1599.

[17] S. Yamamura, S. Nishiyama, *Synlett* **2002**, *4*, 0533–0543.

[18] K. S. Alva, L. Samuelson, J. Kumar, S. Tripathy, A. L. Cholli, *J. Appl. Polym. Sci.* **1998**, *70*, 1257–1264.

[19] L. Michaelis, M. P. Schubert, *Chem. Rev.* **1938**, *22*, 437–470.

[20] M. Z. Wrona, G. Dryhurst, *J. Pharm. Sci.* **1988**, *77*, 911–917.

[21] A. Napolitano, M. d'Ischia, G. Prota, T. M. Schultz, L. J. Wolfram, *Tetrahedron* **1989**, *45*, 6749–6760.

[22] a) B. L. Kindler, P. Spiteller, *Angew. Chem. Int. Ed.* **2007**, *46*, 8076–8078; *Angew. Chem.* **2007**, *119*, 8222–8224; b) J. Caspar, P. Spiteller, *ChemBioChem* **2015**, *16*, 570–573; c) P. Brandt, M. García-Altares, M. Nett, C. Hertweck, D. Hoffmeister, *Angew. Chem. Int. Ed.* **2017**, *56*, 5937–5941; *Angew. Chem.* **2017**, *129*, 6031–6035; d) P. Spiteller, *Nat. Prod. Rep.* **2015**, *32*, 971–993; e) M. Lang, P. Spiteller, V. Hellwig, W. Steglich, *Angew. Chem. Int. Ed.* **2001**, *40*, 1704–1705; *Angew. Chem.* **2001**, *113*, 1749–1751.

[23] M. Leopoldini, T. Marino, N. Russo, M. Toscano, *J. Phys. Chem.* **2004**, *108*, 4916–4922.

[24] R. V. Barbehenn, C. P. Constabel, *Phytochemistry* **2011**, *72*, 1551–1565.

Manuscript received: August 13, 2019
Accepted manuscript online: November 14, 2019
Version of record online: December 4, 2019

